

## NUMERICAL MODELING FOR THE ACCURATE COMPUTATIONS OF ARC-HEATER FLOWS

Jeong-II Lee\*, Chongam Kim† and Kyu-Hong Kim‡

\*Seoul National University,  
Sillim-Dong, Gwanak-Gu, Seoul, Korea  
e-mail: [snow0730@empal.com](mailto:snow0730@empal.com)

†Seoul National University,  
Sillim-Dong, Gwanak-Gu, Seoul, Korea  
e-mail: [chongam@snu.ac.kr](mailto:chongam@snu.ac.kr)

‡Seoul National University,  
Sillim-Dong, Gwanak-Gu, Seoul, Korea  
e-mail: [aerocfd1@snu.ac.kr](mailto:aerocfd1@snu.ac.kr)

**Key words:** Plasma wind tunnel, Arc-Heater, Joule heating, Radiation, Turbulence

**Abstract.** *The purpose of this paper is to develop an accurate analysis code for the flow of arc-heater by employing advanced numerical models. Governing equations are hyperbolic-type axisymmetric Navier-Stokes equations which include joule heating by arc, radiation and turbulent transport effect. Joule heating is simply calculated by Ohm's law with the given distribution of current. Radiation is computed by the three-band model which accounts for self-absorption and is consistent with the detailed line-by-line radiation model. Turbulence effect is incorporated by two-equation turbulence models which can describe the transport of turbulence. In order to assess the performance of the newly developed code, AHF and IHF are calculated in various operating conditions. And, it is confirmed that two-equation turbulence models combined with the three-band radiation model simulate the flow physics in arc-heater more accurately than any other previous models and the influence of the turbulence is as much as or bigger than radiation effect.*

### 1 INTRODUCTION

Since the human being stepped into space, several planetary entry vehicles have been developed and have carried out their mission. When they enter some planets including the earth, they are commonly exposed to tremendous aerodynamic heating which necessitates the thermal protection system (TPS). For that reason, TPS is considered as one of the most important technologies in development of planetary entry vehicles. In addition, its importance is increasing as reusable reentry vehicle is more and more useful.

Recently, various space missions are planned in Europe, Japan, China as well as USA. As a result, the requirement of ground test facility is increasing and many ground test facilities have been developed and are being developed. The representative ground test facility for development of TPS would be a plasma wind tunnel which can provide the high enthalpy

flow for a long time. Among several types of plasma wind tunnel, segmented arc-heater wind tunnel can produce stable and high-quality flow which is an essential requirement as a plasma wind tunnel. For the reliable design of arc-heater, its flow characteristics should be investigated in advance. Flow in arc-heater is complex plasma because the gas is heated directly by arc and the large amount of energy is transferred from the core to the surrounding gas mainly by radiation and turbulent thermal conduction. And, there have been numerous investigations to understand the flow physics numerically and experimentally.

The present paper is concerned with numerical efforts to reveal the flow physics in arc-heated wind tunnel. Historically, Waston *et al.*<sup>1</sup> developed the code which solves parabolic Navier-Stokes equations by the space marching technique in order to analyze the flow in an arc-heater. The optically thin model is applied to describe the radiation. The turbulent effect is considered by a crude algebraic turbulence model. As a result, it was insufficient to describe the flow behavior of arc-heaters accurately. Subsequently, Nicolet *et al.*<sup>2</sup> improved the code by introducing the two-band radiation model that accounts for self-absorption and by modifying the turbulence model. The code was named ARCFLO and it was able to predict the operating characteristics of existing arc-heaters to some extent. However, the characteristics of its radiation model are different from the real physical phenomena, because two absorption coefficients for the radiation model are adjusted empirically by trial and error. Thus, Sakai *et al.*<sup>3,4</sup> improved ARCFLO code by employing the PRG(Planck-Rosseland-Gray) radiation model which may calculate radiative heat fluxes using three mean absorption coefficients. The code could obtain a fairly good agreement with experimental data by tuning a set of the turbulence parameters.

Recently, new CFD codes that solve hyperbolic Navier-Stokes equations by the time marching technique have been developed. Previously developed codes have some serious limitations as a design tool because they are based on the parabolic partial differential equations. For the space marching, flow properties at the upstream of a constrictor should be specified, which cannot be obtained without prior experiments. In order to overcome this defect, Kim *et al.*<sup>5</sup> developed the code, ARCFLO2, which solves hyperbolic Navier-Stokes equations by the time marching technique. They retained the two-band radiation model of ARCFLO and used Cebeci-Smith algebraic turbulence model. ARCFLO2 was applied to arc-heaters at Arnold Engineering Development Center and at Sandia National Laboratory. In order to remove discrepancy between experimental data and calculations, additional viscosity which is a function of current, mass flow rate and geometry is introduced. It was explained that necessity of the additional viscosity originates from inaccuracy in two-band radiation model and the thermal non-equilibrium phenomenon near the wall.<sup>5</sup> Subsequently, Sakai *et al.*<sup>6,7</sup> made an attempt to improve ARCFLO2 and developed a new three-band radiation model which is consistent with the detailed line-by-line radiation calculation. The code was named ARCFLO3 and is applied to 20MW and 60MW arc-jet facilities at NASA Ames Research Center. The results showed good agreements for 60MW arc-heater but relatively poor agreements for 20MW arc-heater. They claimed that poor agreement for 20MW arc-heater is caused by non-equilibrium flow properties.<sup>7</sup>

Previous researchers<sup>5,6,7</sup> suggested that it is necessary to study new effects such as non-equilibrium phenomenon. However, there is still a room to improve existing numerical

models. Progress has been continuously made in the field of radiation<sup>2,3,4,6,7</sup> but turbulent effect is relatively not investigated in detail<sup>5,8</sup>. Until now, good agreements between experiment and calculation could be obtained by tuning a set of the turbulence parameter and the wall roughness, or by directly controlling the magnitude of turbulence like the additional viscosity for the specific arc-heater. If these models are applied to other arc-heaters with the same tuning parameters, accuracy tends to lose. This behavior is mainly caused by the role of turbulence model which profoundly influences on the flow physics of the arc-heater.

The purpose of this paper is to develop an accurate analysis code which can design new arc-heaters. In order to accomplish the goal, the code should show reasonable solutions in general flow conditions and should not possess empirical or adjusting factors based on user's experience. Thus, we adopt the latest numerical model of radiation and turbulence, which could guarantee reasonable accuracy in general flow conditions.

In the present paper, three-band radiation model which is consistent with the detailed line-by-line radiation calculation is adopted, and two-equation turbulent models to avoid the defects of algebraic turbulent model are used for the accurate prediction of the real flow in arc-heater. Then, the 20MW Aerodynamic Heating Facility (AHF) and 60MW Interaction Heating Facility (IHF) at NASA Ames Research Center are investigated. The results show a good agreement with experimental data for all arc-heaters. It is confirmed that k- $\epsilon$  turbulence model combined with three-band radiation model is appropriate for the flow analysis in arc heaters. It also shows that the influence on the heat transfer mechanism by the turbulence is as much as or bigger than radiation effect.

## 2 NUMERICAL MODELING

### 2.1 Governing equations

Arc-jet wind tunnel is classified variously according to the type of arc-heater. Figure 1 shows a segmented constrictor type arc-heater which is used widely. It consists of an anode chamber, a constrictor, a cathode chamber and a nozzle. Most test gas is injected through the wall of constrictor and exits through a nozzle into a test section. In the constrictor, arc spans between two electrodes. The core gas is heated directly by the joule heating due to arc and the surrounding gas is heated by radiation emitted from the core gas and by turbulent mixing. And the heat energy which arrived at the constrictor wall is removed immediately by the cooling water which circulates through constrictor disks.

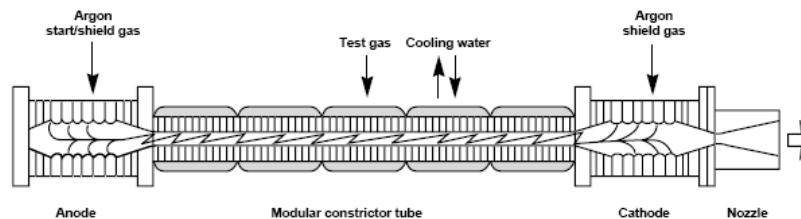


Figure 1: Schematic drawing of the segmented arc-heater

In order to calculate such a flow, the governing equations are chosen as hyperbolic-type axisymmetric Navier-Stokes equations which include the joule heating by arc, radiation and turbulent transport effect, which are written as follows in a vector form.

$$\frac{\partial \mathbf{Q}}{\partial t} + \frac{\partial \mathbf{E}}{\partial x} + \frac{\partial \mathbf{F}}{\partial x} + \mathbf{H} = \frac{\partial \mathbf{E}_v}{\partial x} + \frac{\partial \mathbf{F}_v}{\partial x} + \mathbf{H}_v + \mathbf{I} \quad (1)$$

where,

$$\mathbf{Q} = \begin{bmatrix} \rho \\ \rho u \\ \rho v \\ \rho e_t \end{bmatrix}, \quad \mathbf{I} = \begin{bmatrix} 0 \\ 0 \\ 0 \\ -j \cdot E \end{bmatrix}, \quad \mathbf{H} = \frac{1}{y} \begin{bmatrix} \rho v \\ \rho uv \\ \rho v^2 + p \\ \rho H v \end{bmatrix}, \quad \mathbf{H}_v = \frac{1}{y} \begin{bmatrix} 0 \\ \tau_{xy} \\ \tau_{yy} - \tau_{\theta\theta} \\ u\tau_{xy} + v\tau_{yy} - q_{c,y} - q_{R,y} \end{bmatrix},$$

$$\mathbf{E} = \begin{bmatrix} \rho u \\ \rho u^2 + p \\ \rho uv \\ \rho Hu \end{bmatrix}, \quad \mathbf{F} = \begin{bmatrix} \rho v \\ \rho uv \\ \rho v^2 + p \\ \rho H v \end{bmatrix}, \quad \mathbf{E}_v = \begin{bmatrix} 0 \\ \tau_{xx} \\ \tau_{xy} \\ u\tau_{xx} + v\tau_{xy} - q_{c,x} - q_{R,x} \end{bmatrix}, \quad \mathbf{F}_v = \begin{bmatrix} 0 \\ \tau_{xy} \\ \tau_{yy} \\ u\tau_{xy} + v\tau_{yy} - q_{c,y} - q_{R,y} \end{bmatrix} \quad (2)$$

The gas is assumed to be chemically equilibrium. The thermodynamic properties such as pressure and temperature are calculated using curve fitting data.<sup>9</sup> The transport properties such as viscosity and thermal conductivity are calculated also using curve fitting data.<sup>10</sup> The available temperature range is 500k~30000k, and pressure range is  $10^{-4} \sim 10^2$  atm.

## 2.2 Numerical schemes and boundary conditions

Governing equations are discretized using the finite volume method. The inviscid flux is given by the AUSMPW<sup>11</sup> flux and the viscous flux is calculated through a central difference scheme. The inviscid term is handled implicitly by applying LU-SGS (Lower Upper Symmetric Gauss Seidel). The axisymmetric source, joule heating and viscous term are calculated explicitly.

For wall boundary conditions, the air which is injected from gaps between adjacent constrictor disks are considered as a mass flow source distributed uniformly over the side wall.<sup>5</sup> Wall temperature is fixed at 1100K and density at the wall is determined by the equilibrium relation among wall temperature and pressure.<sup>5</sup> the outlet condition is extrapolated from the value of the inner computational domain because the region behind nozzle throat is supersonic.

## 2.3 Joule heating modeling

Generally Joule heating by arc should be calculated by solving Maxwell equation. However, if the distribution of current is known, it can be calculated simply by Ohm's law. Fortunately, a current in the constrictor is constant, because the wall of constrictor is insulated electrically. Thus, with assumption that the voltage gradient is independent of a radius, Joule heating can be simply calculated as follows.

Ohm's law for a cylindrical column is

$$j(x, y) = \sigma(x, y) \cdot E(x), \quad (3)$$

$$E(x) = \frac{j(x, y)}{\sigma(x, y)} = \frac{\int_0^R 2\pi y j(x, y) dy}{\int_0^R 2\pi y \sigma(x, y) dy} = \frac{I}{\int_0^R 2\pi y \sigma(x, y) dy} \quad (4)$$

where

$$I = \int_0^R 2\pi y j(x, y) dy = \text{const} \quad (5)$$

from Kirchoff's law of conservation of current.

Finally joule heating is given as

$$j(x, y) \cdot E(x) = \frac{I^2 \sigma(x, y)}{\left[ \int_0^R 2\pi y \sigma(x, y) dy \right]^2} \quad (6)$$

where the electrical conductivity is taken from the reference 2.

Figure 2 shows the current distribution along the axial direction.

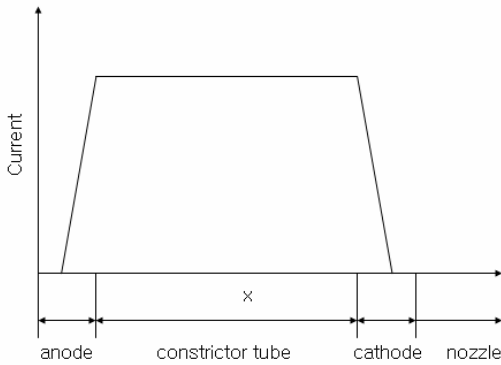


Figure 2: Current distribution in the arc-heater

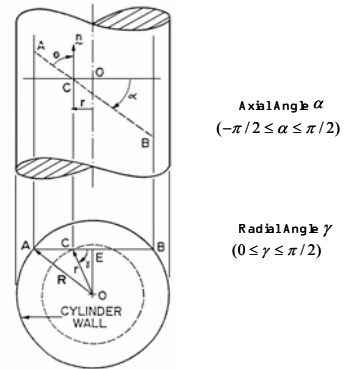


Figure 3: Cylindrical geometry and coordinate system

## 2.4 Radiation modeling

At high temperature flows, the radiation is an important mode of heat transfer together with thermal convection. So, the radiant heat transfer term should be included in energy equation. In order to calculate this, the radiative transfer equation in cylindrical coordinates should be solved and is written as follows

$$-\frac{1}{\rho \kappa_v} \frac{dI_v}{ds} = I_v - B_v, \quad (7)$$

where  $I_v$  is radiative intensity traveling along a ray. Absorption coefficient  $\kappa_v$  is function of frequency, temperature and pressure, which is gained from experiments. Planck function

$B_\nu$  is written as follows

$$B_\nu = \frac{2h}{c^2} \frac{\nu^3}{e^{h\nu/kT} - 1}. \quad (8)$$

When the radiative intensity at a given point in the gas is calculated for all directions, then the radiant flux per unit frequency at radius  $r$  can be obtained as

$$q_\nu(r) = \int_{\Omega} I_\nu(r) \cos \theta d\Omega. \quad (9)$$

The total radiant flux, integrated over all frequency, is calculated as

$$q_R(r) = \int_0^\infty q_\nu(r) d\nu. \quad (10)$$

By the application of the concept of a multi-band model, the total radiant flux is written as

$$q_R(r) = \sum_n q_n(r). \quad (11)$$

To calculate radiation accurately, line-by-line calculation<sup>12</sup> is most desirable. However computing time for such a calculation is extremely large. So, Sakai *et al.*<sup>7</sup> developed new three-band model. This model computed the radiative transport equation 400 times faster than a detailed line-by-line calculation without sacrificing the accuracy of the detailed calculation. In this model, three absorption coefficients which are defined at a given wavelength are functions of pressure and temperature over the pressure ranges from 1 atm to 10 atm and the temperature ranges from 1000K to 15000K. In the present work, three-band radiation model<sup>7</sup> are adopted to describe accurately the radiative flow physics in arc-heaters.

## 2.5 Turbulence modeling

Turbulence is one of the key phenomena in arc-heater flow. Traditionally, algebraic turbulence models are used for its analysis. These models are equation wherein the turbulent fluctuating correlations are related to the mean flow quantities by algebraic relations. They are the simplest to implement of all turbulence models and rarely cause unexpected numerical difficulties. However, these models do not include the convection effect of turbulence,<sup>14</sup> because underlying assumption in these models is that the local rate of production of turbulence and the rate of dissipation of turbulence are approximately equal. Furthermore, because these models work well only for the flows for which they have been fine tuned, it is difficult to extrapolate beyond the established data base for which an algebraic model is calibrated.<sup>16</sup>

In arc-heater, flow is complex because gas is injected perpendicularly through the wall of constrictor and impinges against the flow on the opposite side. And flow is strong turbulence which is produced by gas injections continuously and is convected and diffused fast along the flow. Therefore, coefficients of algebraic models should be tuned precisely for arc-heater flows. However, because such precise tuning is arrived at a long series of trial and error involving experiments, it is necessary to introduce more advanced turbulence models that

have less empirical turbulence coefficients which are well tuned and can describe transport of turbulent flows in detail. Furthermore, the algebraic models used for the analysis of arc-heater flows require information regarding the boundary layer thickness and flow properties at the boundary edge, but it is difficult to define them accurately due to impinging flow near the core region. In real calculations, they are defined as properties at the core, but could be different from real values.

In present study, three two-equation turbulence model, that is, k- $\epsilon$  model of Jones and Launder<sup>15</sup>, k- $\omega$  model of Wilcox<sup>16</sup>, and k- $\omega$  SST model of Menter<sup>17</sup> are tested as advanced turbulence models. They are currently most popular models which solve a transport equation for the turbulence kinetic energy. And they can be used to predict properties of a given turbulent flow with no prior knowledge of the turbulence structure.<sup>14</sup> However, these turbulent models have different performance as the characteristic of flow.<sup>18</sup> The k- $\epsilon$  model of Jones and Launder is the most widely known and extensively used two-equation eddy viscosity model. For wall bounded flows, the model gives good agreement with experimental results for zero and small mean pressure gradients, but is less accurate for large adverse pressure gradients. The k- $\omega$  model of Wilcox is a well known and widely tested two-equation eddy viscosity model. This model has proven to be superior in numerical stability to the k- $\epsilon$  model primarily in the viscous sublayer near the wall. However, the results of the k- $\omega$  model are sensitive to small freestream values of  $\omega$ . The k- $\omega$  SST model of Menter combines several desirable elements of k- $\epsilon$  model and k- $\omega$  model. This model incorporates k- $\omega$  model near solid walls and it switches to k- $\epsilon$  model near boundary layer edges and in free-shear layers. The shear stress transport(SST) modification improves the prediction of flows with strong adverse pressure gradients and separation.

### 3 RESULTS

In this study, three-band radiation model and two equation turbulence model are coupled with the governing equations to describe the mechanism of heat transfer accurately in the arc-heater. Calculations have been carried out for following two sets of experimental data, data of the 20MW Aerodynamic Heating Facility(AHF) and 60MW Interaction Heating Facility(IHF) at NASA Ames Research Center. After the calculation, basic performance parameters, that is, the voltage between electrodes, mass averaged enthalpy at the nozzle throat, pressure in the cathode chamber, and the heater efficiency are compared with the experimental data. Mass-averaged enthalpy and efficiency are defined as follows.

Mass-averaged Enthalpy(J/kg) :

$$H_a(x) = \frac{\int_0^R 2\pi y \rho(x, y) u(x, y) H(x, y) dy}{\int_0^R 2\pi y \rho(x, y) u(x, y) dy} . \quad (12)$$

Efficiency(%) :

$$\eta = \frac{\text{power absorbed by flow}}{\text{power input}} = 100 \times \left( 1 - \frac{q_R - q_c}{I \cdot V} \right) . \quad (13)$$

The dimensions of the arc-heater are obtained from reference 7. The dimensions of constrictor and nozzle throat are directly obtained, but the geometry of electrode chambers is unknown, so it is obtained by using a computer program which digitizes points of scanned grid images. The AFH arc-heater has a constrictor diameter of 0.06m and length of 2.3m. The nozzle throat diameter is 0.038m. And the IFH arc-heater has a constrictor diameter of 0.08m, length of 3.9m and nozzle throat of 0.0603m. The computation grids which are scaled up to 10 times in radial direction are shown in Figure 4.

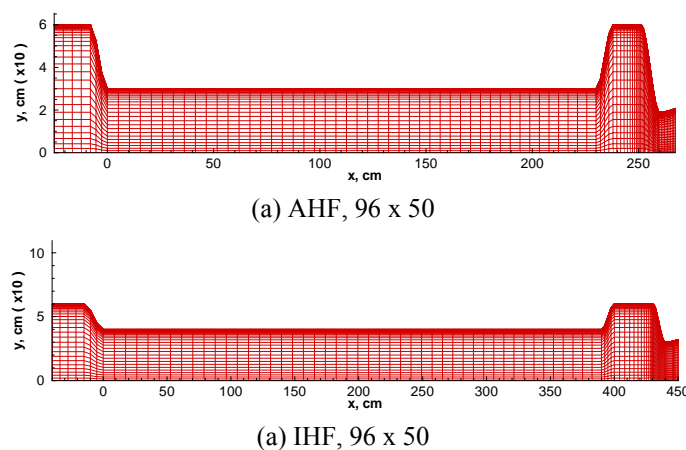


Figure 4: Grid systems

### 3.1 Comparison with AHF data

The AHF can operate with either a 20MW constricted arc-heater or a Hules arc-heater. Most of the testing in the AHF is done by using the segmented arc heater because of its high enthalpy performance, low stream contamination, and long history of repeatable operation. The constricted arc-heater operates at pressure from 1 to 9 atm and enthalpy levels from 1 to 33 MJ/kg.

Recently, Hightower et al. performed a series of arc-jet tests in the AHF by the energy balance method.<sup>13</sup> Sakai et al. computed those flows by using ARCFLO3 code and compared their results with Hightower's experimental data.<sup>7</sup> In Sakai's study, ARCFLO3 code solved the mixture of air and small amount of argon by using a three-band radiation model and an algebraic turbulence model.

In this study, the comparison between computation and experiment is made for the AHF arc-heater like Sakai's study. The computed results for voltage, mass-averaged enthalpy, chamber pressure and efficiency are compared with experiments. The data are presented for the case of  $I=1600A$  and  $2000A$ , respectively. And the data are plotted against the mass flow rate. Figure 5 shows results for  $I=1600A$ . As shown in figures, calculated results using  $k-\epsilon$  turbulence model are most accurate. The computation predicts mass-averaged enthalpy and efficiency within the scatter of the experiment. The calculated voltage is most accurate in various flow conditions. And the calculated chamber pressure shows a good agreement. For the case of  $k-\omega$  turbulence model and  $k-\omega$  SST turbulence model, a qualitative trend of the

calculated results is similar to that of experiment, but some calculated data are slightly different from the experimental data. For the case of  $k-\omega$  turbulence model, the computation overestimates mass-averaged enthalpy and efficiency over all mass flow rates. For the case of  $k-\omega$  SST turbulence model, the computation predicts lower voltage and higher efficiency. Figure 6 shows results for  $I=2000A$ . The results show the same tendency as those for  $I=1600A$ . The computation using  $k-\epsilon$  turbulence model predicts most accurately. Many calculated data are located within scattered experimental data. However, for the case of  $k-\omega$  turbulence model and  $k-\omega$  SST turbulence model, some calculated data are slightly different from experimental data.

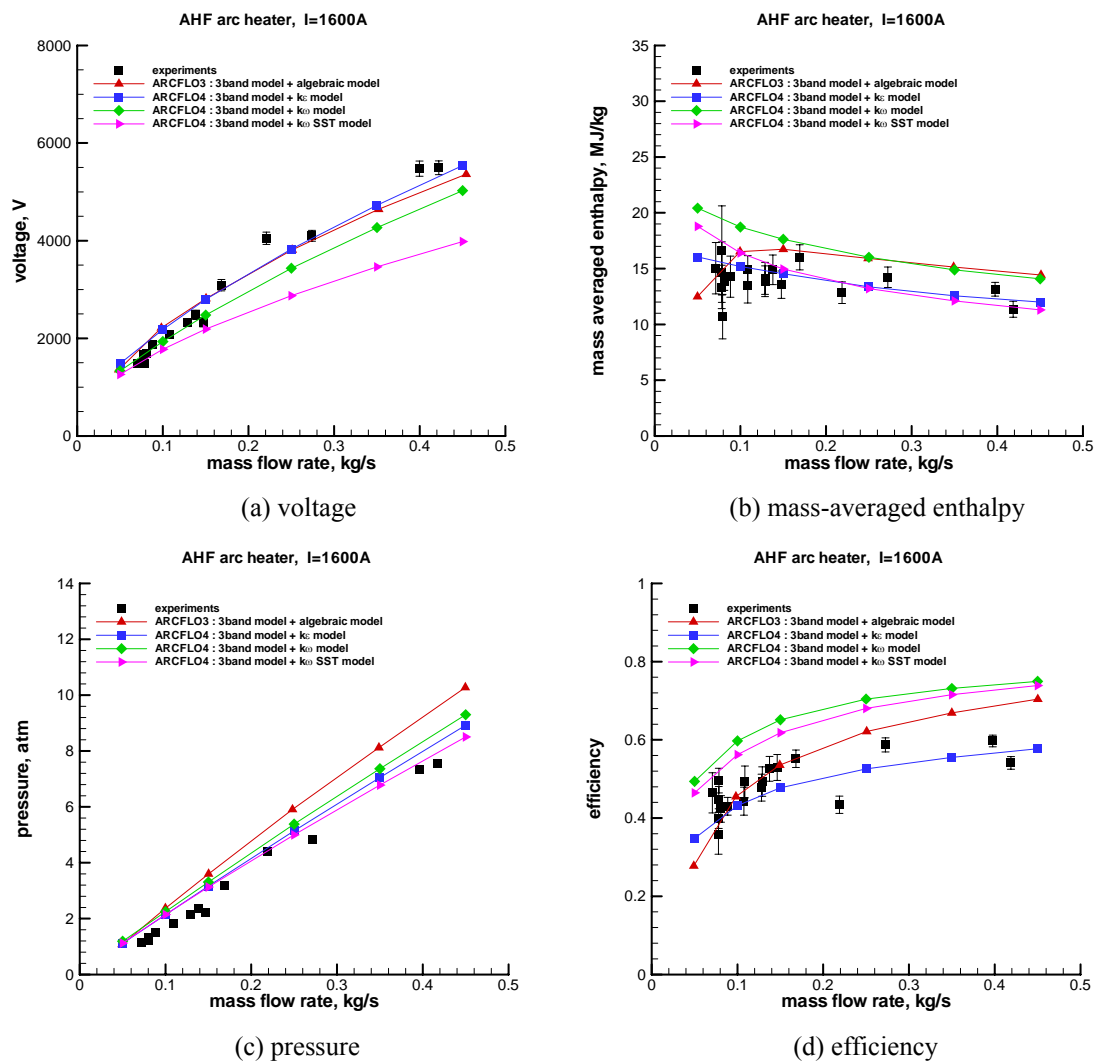


Figure 5: Comparison between calculations and experiments for AHF ( $I=1600A$ )

Based on the computation for AHF arc-heater, one can see that the turbulence phenomena

in arc-heater are very different as the turbulence models and more accurate solution can be obtained by improving the turbulence model. In this study,  $k-\varepsilon$  turbulence model predicts the flow characteristics of AHF arc-heater most accurately.

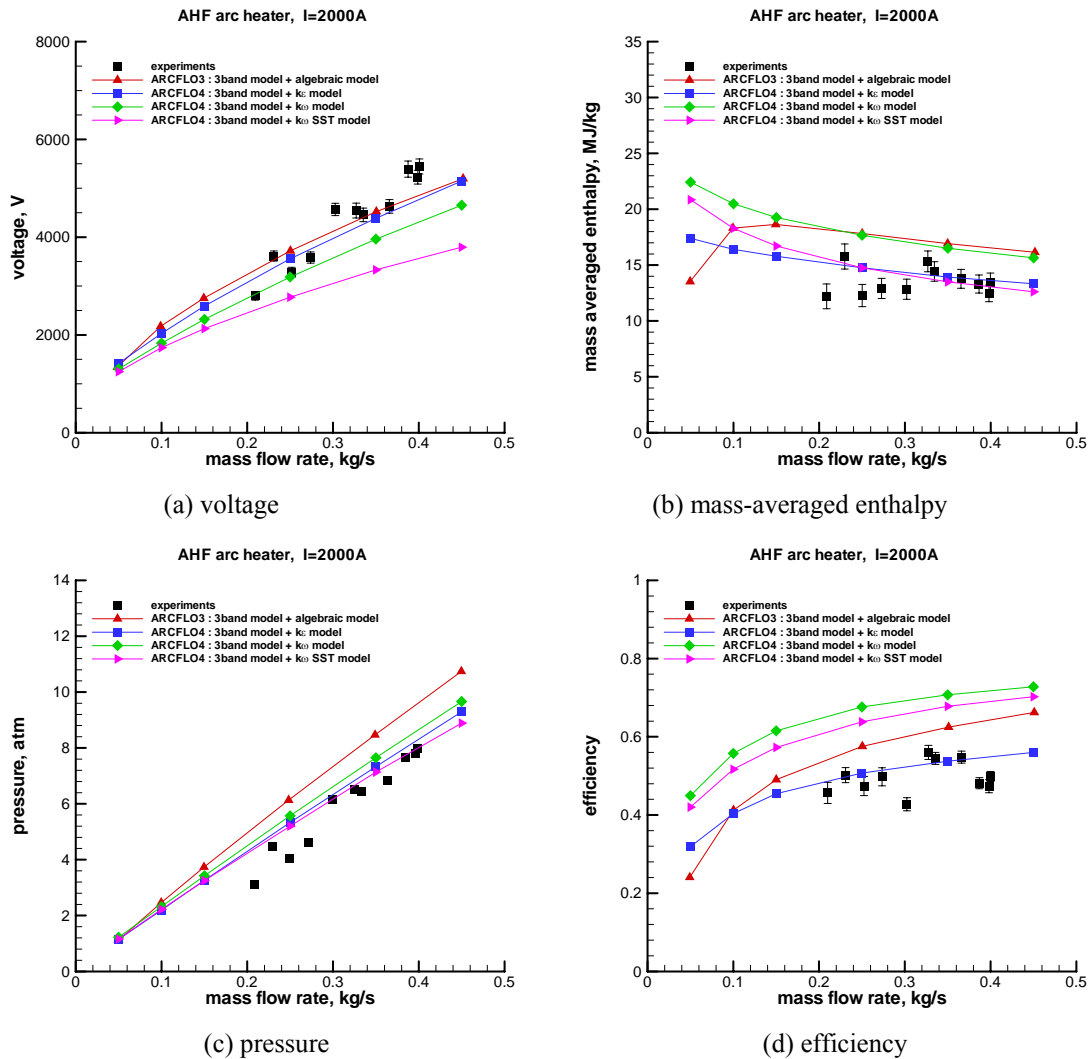


Figure 6: Comparison between calculations and experiments for AHF ( $I=2000A$ )

### 3.2 Comparison with IHF data

The IHF is equipped with a 60 MW constricted heater that operates at pressures from 1 to 9 atm and enthalpy levels from 7 to 47 MJ/kg. Recently, arc-jet tests in the IHF were performed by Hightower et al. and the flows were computed by Sakai et al.<sup>7</sup>

As in previous section, calculated results are compared with Sakai's calculated data as well as experimental data. The results, which are plotted against mass flow rate, are presented for the case of  $I=3000A$  and  $6000A$ , respectively. Figure 7 shows calculated and experimental

data for  $I=3000A$ . Like the results of AHF, the computation using  $k-\epsilon$  turbulence model predicts voltage, mass-averaged enthalpy, chamber pressure and efficiency accurately. Most computed data are within the error bar for the experimental data, and only a few data are around error bar. For the case of  $k-\omega$  turbulence model, the computation predicts voltage and chamber pressure accurately, but overestimates mass-averaged enthalpy and efficiency. For the case of  $k-\omega$  SST turbulence model, the results show a fair agreement for mass-averaged enthalpy and chamber pressure, but a poor agreement for voltage and efficiency. Figure 8 shows results for  $I=6000A$ . The results have the same tendency as those for  $I=3000A$ . As shown in figures, calculated results using  $k-\epsilon$  turbulence model agree well with experimental data. However, some computations for  $k-\omega$  turbulence model and  $k-\omega$  SST turbulence model are slightly different from experiment.

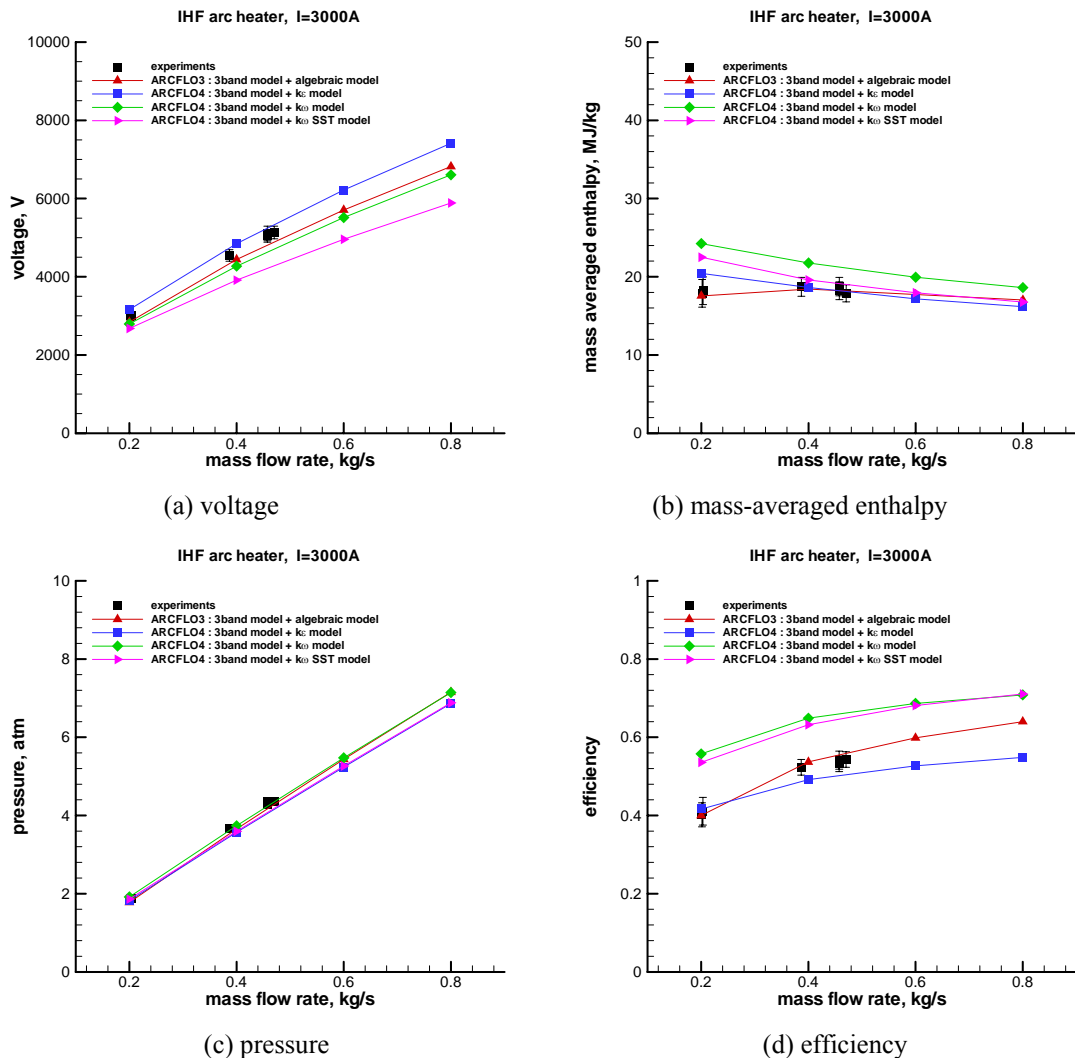
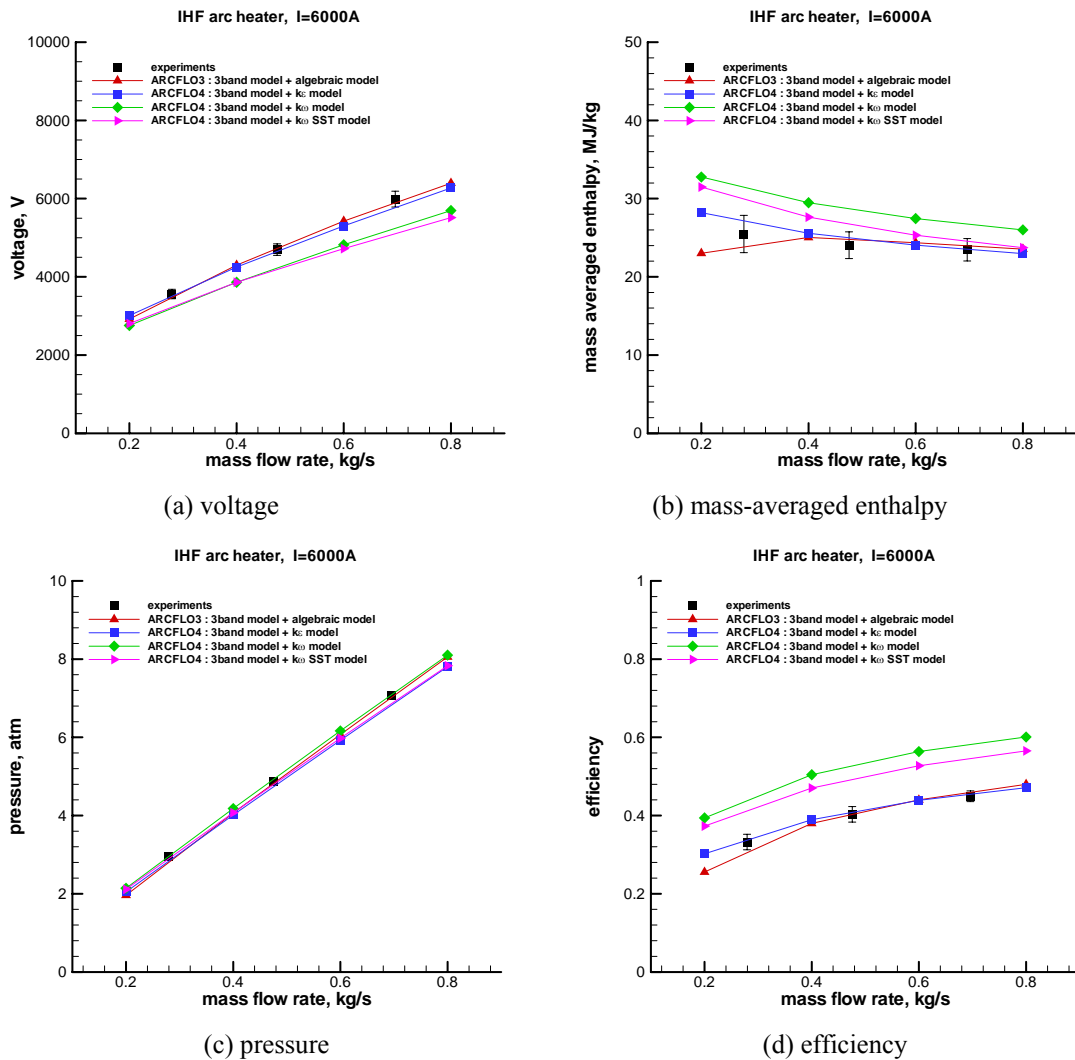


Figure 7: Comparison between calculations and experiments for IHF ( $I=3000A$ )


 Figure 8: Comparison between calculations and experiments for IHF ( $I=6000A$ )

This computation, like that of the AHF arc-heater, shows that  $k-\epsilon$  turbulence model describes flow in arc-heater accurately. So, combination of  $k-\epsilon$  turbulence models and a three-band radiation model seems to be more general than that of models used in previous codes.

### 3.3 Comparison of heat transfer between radiation and turbulence

From precious results, the computation using  $k-\epsilon$  model shows better agreement with the experiment than that of other models. To find the reason, turbulence viscosity and turbulent heat flux are compared according to turbulence models. Figure 9 and 10 show distributions of turbulent viscosity and turbulent heat flux in radial direction at the constrictor end of AHF arc-heater. In figure 9, the calculation using  $k-\epsilon$  model predicts the highest turbulent heat flux, since this turbulence model has the highest viscosity on all radial location. Therefore

calculated mass-averaged enthalpy and efficiency by using  $k-\epsilon$  model become lower than those by using other turbulence models as shown in figure 5(b) and (d). That is, high turbulent heat flux at the downstream decreases mass-averaged enthalpy and efficiency. This tendency is shown in computation of IHF. In figure 10, the calculation using  $k-\epsilon$  model predicts highest viscosity and heat flux. Therefore in figure 7(b) and (d) mass-averaged enthalpy and efficiency for  $k-\epsilon$  model are lowest among calculated data for two-equation models.

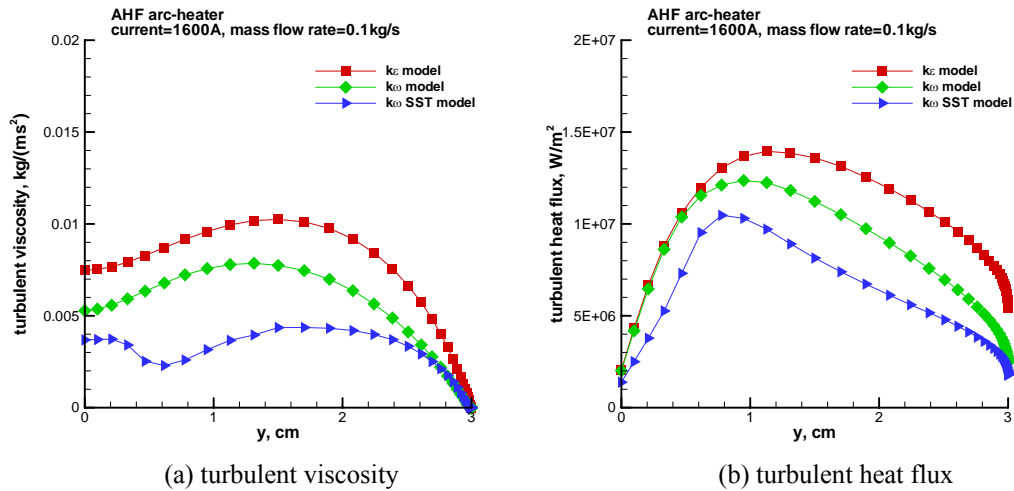


Figure 9: Comparison between turbulence models (AHF)

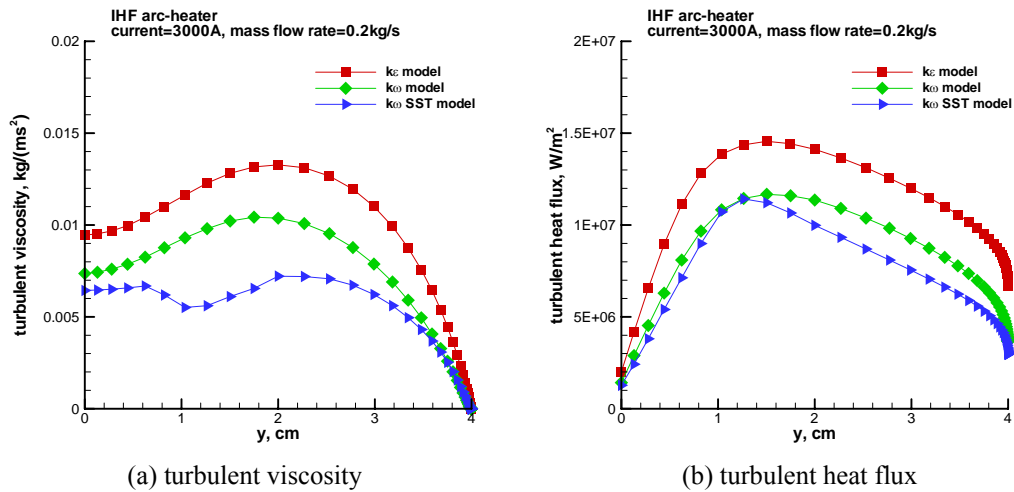


Figure 10: Comparison between turbulence models (IHF)

The way to increase the accuracy by enhancement of the heat flux is shown in Kim's and Sakai's study too. Kim et al. enhanced the heat transfer by introducing the additional viscosity and Sakai et al. made heat flux increase by using sand grain roughness model. However the effect of additional viscosity and roughness is not the cause of the discrepancy, because they

can predict flow physics accurately for only limited cases where their coefficients were tuned.

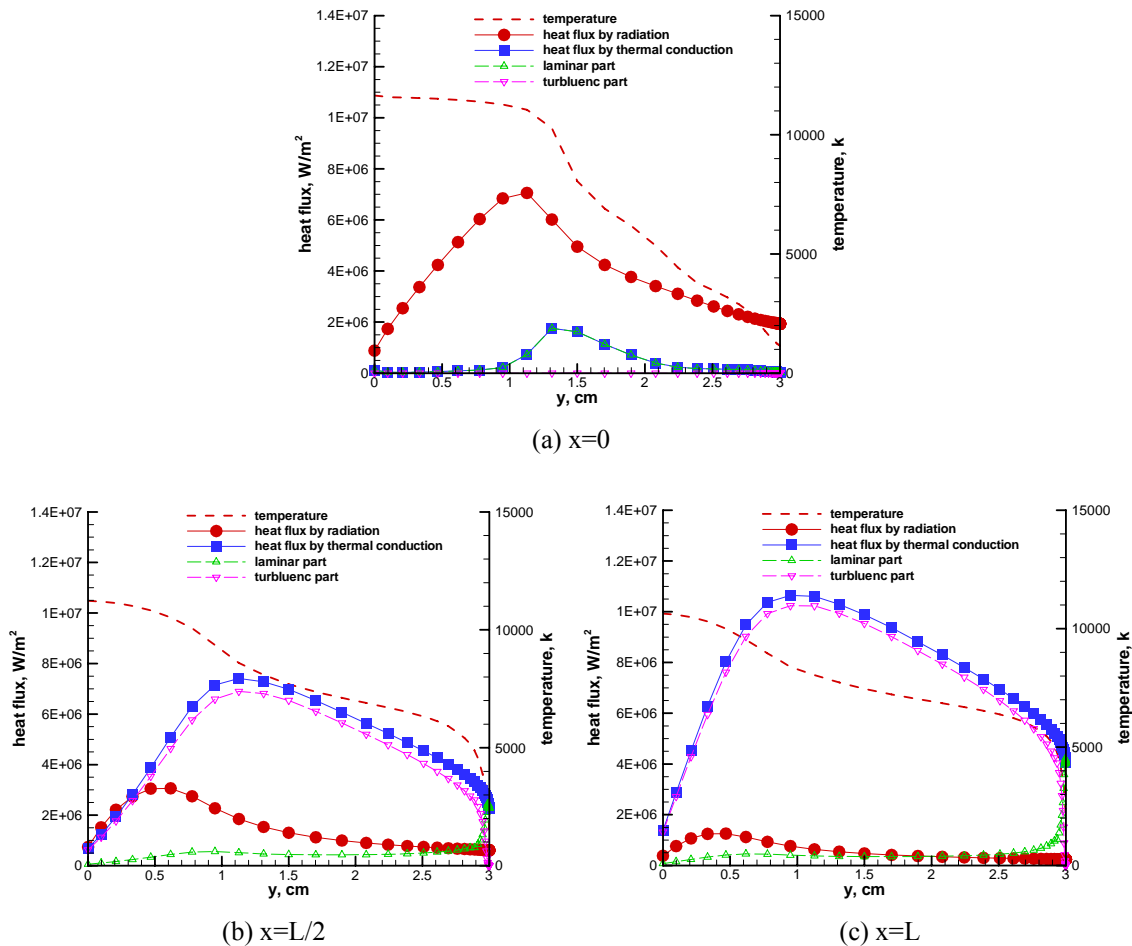


Figure 11: Heat transfer mechanism in the constrictor (AHF,  $I=1600A$ , mass flow rate = 0.1 kg/s)

### 3.4 Comparison of heat transfer between radiation and turbulence

Flow characteristics in arc-heater depend on the mechanism that the heat is transferred from the core to the surrounding. It is known that most heat energy is transferred by the radiation and the turbulence. It is necessary to compare the heat absorption by the radiation and the turbulence to check how the turbulence has influence on the flow in arc-heater. Figure 11 shows the heat flux along the radial direction at the beginning, the middle, and the end of constrictor, when the  $k-\epsilon$  model is used. The heat absorption can be defined as the difference of the flux in a cell. So, the positive gradient means that the gas absorbs heat energy and the negative gradient means that the gas emits or loses the heat energy. In figure 11(a), the heat flux by the radiation is bigger than that by the turbulence. Core region gas emits much heat energy by the radiation, and the energy is absorbed by surrounding gas or transferred to constrictor wall. Figure 11(b) shows that the heat absorption and loss by the turbulence are

more than those by the radiation at the middle of constrictor. In comparison with the beginning of constrictor, the heat absorption and loss by the radiation decrease, while those by the turbulence increase. In figure 11(c), the heat absorption and loss by the radiation is very small. Most of heat absorption and loss are made by the turbulence. These figures show that the influence by the radiation decreases and that by the turbulence increases as the flow goes to rear region. As shown in figure 12, this phenomenon becomes clear as mass flow rate injected from the wall is increased. The figure shows that as mass flow rate is increases the influence by the turbulence becomes larger.

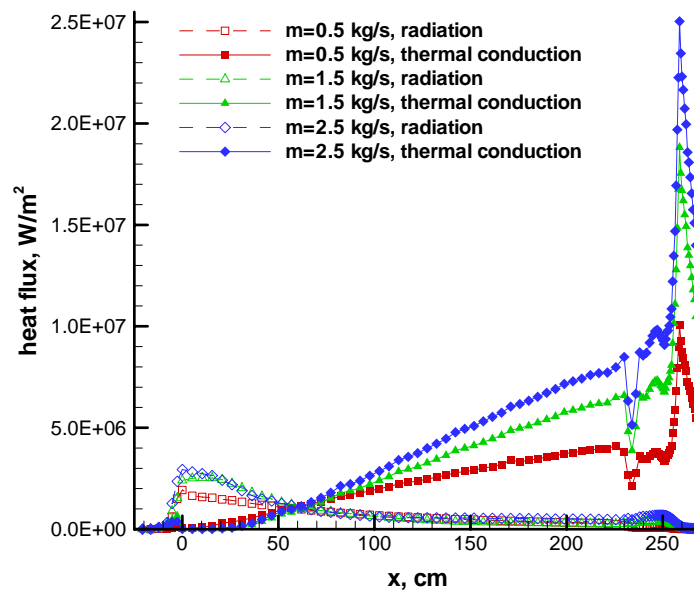


Figure 12: Comparison of heat flux at the wall of the arc-heater (AHF, I=1600A)

#### 4 CONCLUSION

Purpose of this paper is to find generalized numerical models for accurate analysis of arc-heater flows. Until now, some researchers successfully calculated the inner flows of a specific arc-heater, but could not present proper numerical models which satisfy common operating conditions for various arc-heaters. Many studies were mainly focused on the radiation modeling. Only some progress has been made in the consideration of turbulent effect. The turbulence model should be improved as well as radiation model for the accurate prediction.

In this work, generalized numerical models are adopted to analysis flow accurately in various conditions of arc-heaters. The radiation is computed by a three-band model which accounts for self-absorption and is consistent with a detailed line-by-line radiation calculation. And the turbulence is described by two-equation turbulence models which can express the transport of turbulence. The flow analysis of arc heaters such as the 20MW Aerodynamic Heating Facility (AFH) and 60MW Interaction Heating Facility (IHF) at NASA Ames

Research Center has been carried out. Based on these computations, it is confirmed that  $k$ - $\epsilon$  turbulence model and three-band radiation model are appropriate to analysis more accurately the physics of arc-hear flow in various conditions. And the comparison of the heat flux between the radiation and the turbulence is performed. It shows that the influence on the heat transfer mechanism by the turbulence is as much as or bigger than that by the radiation.

## ACKNOWLEDGMENT

The authors would like to acknowledge the support from KISTI (Korea Institute of Science and Technology Information) under The Strategic Supercomputing Support Program with Dr. Sang Min Lee as the technical supporter. The use of the computing system of the Supercomputing Center is also greatly appreciated.

## REFERENCES

- [1] Watson, V. R., and Pegot, E. B., "Numerical Calculations for the Characteristics of a Gas Flowing Axially Through a Constrictor Arc," NASA TN D-4042, 1966
- [2] Nicolet, W. E., Shepard, C. E., C. E., Clark, K. J. Balakrishnan, A., Kesselring, J. P., Suchsland, K. E., and Reese, J. J., "Analytical and Design Study for a High-Pressure, High-Enthalpy Constricted Arc Heater," Arnold Engineering Development Center, AEDC-TR-75-47, Arnold AFB, TN, 1975.
- [3] Sakai, T., Sawada, K., and Park, C., "Assessment of Planck-Rosseland-Gray model for Radiation Shock Layer," AIAA paper 97-2560, June, 1997.
- [4] Sakai, T., Sawada, K., and Mitsuda, M., "Application of Planck-Rosseland-Gray Model for High Enthalpy Arc Heaters," AIAA Journal of Thermophysics and Heat Transfer, Vol. 15, No. 2, 2001, pp. 176-183.
- [5] Kim, K. H., Rho, O. H., and Park, C., "Navier-Stokes Computation of Flows in Arc Heaters," AIAA Journal of Thermophysics and Heat Transfer, Vol. 14, No. 2, 2000, pp. 250-258.
- [6] Sakai, T., and Olejniczak, J., "Navier-Stokes Computations for Arcjet Flows," AIAA Paper 2001-3014, June, 2001.
- [7] Sakai, T., and Olejniczak, J., "Improvement in a Navier-Stokes Code for Arc Heater Flows," AIAA Paper 2003-3782, June, 2003.
- [8] Lee, J. I., Kim, K. H., Kim, C., and O. Rho, "Investigation of Turbulent Flow Effect in Segmented Arc Heater," AIAA Paper 2005-172, January 2005.
- [9] Srinivasan, S., Tannehill, J. C., and Weilmuenster K. J., "Simplified Curve Fits for the Thermodynamic Properties of Equilibrium Air," NASA RP-1181, Aug. 1987
- [10] Gupta, R. N., Lee, K. P., Thompson, R. A., and Yos, J. M., "Calculations and Curve Fits of Thermodynamics and Transport Properties for Equilibrium Air to 30000 K," NASA RP-1260, 1991

- [11] Kim, K. H., Kim, C., and Rho, O. H., "Methods for the Accurate Computations of Hypersonic Flows: I. AUSMPW+ Scheme," *Journal of Computational Physics*, Vol. 174, November 2001, pp. 38-80.
- [12] Whiting, E. E., Park, C., Liu, Y., Arnold, J. O., and Paterson, J. A., "NEQAIR96, Nonequilibrium and Equilibrium Radiative Transport and Spectra Program: User Manual," NASA Reference Publication 1389, December 1996.
- [13] Hightower, T. M., Balboni, J. A., MacDonald, C. L., Anderson, K. F., and Martinez, E. R., "Enthalpy by Energy Balance for Aerodynamic Heating Facility at NASA Ames Research Center Arc Jet Complex," 48th International Instrumentation Symposium, the Instrumentation, Systems, and Automation Society, Research Triangle Park, NC, 2002.
- [14] Hoffmann, K. A., and Chiang, S. T., "Computational Fluid Dynamics Volume III," Engineering Education System, Fourth Edition, 2000.
- [15] Jones, W. P., and Launder, B. E., "The Prediction of Laminarization with a Two-Equation Model of Turbulence," *International Journal of Heat and Mass Transfer*, vol. 15, 1972, pp. 301–314.
- [16] Wilcox, D. C., "Turbulence Modeling for CFD," DCW Industries, Second Edition, 1998.
- [17] Menter, F. R., "Two-Equation Eddy Viscosity Turbulence Models for Engineering Applications," *AIAA J.*, vol. 32, Nov. 1994, pp. 1299–1310.
- [18] Bardina, J. E., Huang, P. G., and Coakley, T. J., "Turbulence Modeling Validation, Testing, and Development," NASA Technical Memorandum 110446, 1997.